Grid-based quantum Monte-Carlo method for fermion systems

Alexander A. Kunitsa

Department of Chemistry, University of Illinois at Urbana-Champaign,

600 South Matthews Ave, Urbana, Illinois, 61801, USA

We present an extension of the diffusion Monte-Carlo algorithm for simulating the quantum states of the few-fermion systems beyond the fixed node approximation. We show that the negative sign problem can be addressed by confining sign-carrying random walkers to the points of a uniform infinite spatial grid, allowing them to meet and annihilate to establish the nodal structure of the target state. The walker dynamics is governed by the imaginary time propagator, derived from an approximate discretized Hamiltonian and can be described as a non-gaussian branching random walk. The accuracy of the resulting stochastic representation of a fermion wave function is only limited by the resolution of a grid and imaginary time-step and can be improved in a controlled manner. We illustrate the method performance for a series of model problems including fermions in harmonic traps as well as the He atom in its singlet and triplet ground states. For the latter case, the Monte-Carlo energy estimates were obtained with sub-millihartree statistical error without invoking the importance sampling transformation, yet were subject to a $\sim$ 15 mH bias due to the inherent inefficiency of the uniform grid in representing rapid variation of the wave function in the core region.

I. INTRODUCTION

Stochastic algorithms hold a potential to improve performance of the correlated real space electronic structure models by addressing the problem of dimensionality inherent in such methods. Real space second-order Møller-Plesset perturbation theory in either original [1] or explicitly correlated formulation [2, 3] as well as real space coupled cluster methods with single and double excitations [4] describe electron correlation in terms of two-particle pair functions satisfying inhomogeneous partial differential equations of Sinanoglu type [1]. Numerical approaches commonly applied to obtain solutions of the equations, rely on the grid

expansions [2–7] of the target six-dimensional quantities and suffer from memory overheads. State of the art quantum Monte-Carlo methods [8–10] are well suited for tackling dimensionality problem, however, most of the well-established algorithms (except for lattice regularized Diffusion Monte-Carlo, LRDMC [11, 12]) are inapplicable in a grid-based setting and make use of the fixed-node approximation [9, 13, 14] to avoid the negative sign problem [15]. The latter critically relies on the availability of the high-quality trial wave functions and can introduce non-systematic errors in calculated energies.

The objective of this work is to extend the Diffusion Monte-Carlo (DMC) method [9] for sampling discretized wave functions expanded on infinite Cartesian grids beyond the fixed-node approximation. Similar to LRDMC, our algorithm relies on a finite difference approximation for the kinetic energy operator to represent the molecular Hamiltonian on the infinite uniform grid, yet does not impose nodal constraints [9, 13, 14] to ensure the convergence of the Monte-Carlo iterations to the target state with correct fermion node. Instead, the nodal structure is established by propagating sign carrying random walkers and performing their cancellation by analogy with Full Configuration Interaction Quantum Monte-Carlo (FCIQMC) [16, 17]. This feature distinguishes our method from previously developed fermion Monte-Carlo approaches that enforce cancellation by walker pairing, correlated dynamics and other techniques [18–24]. Grid-based simulation setup renders the collision probabilities of the walkers with opposite signs non-zero and gives rise to an unbiased cancellation scheme. The typical population dynamics pattern observed in our simulations is identical to that of FCIQMC and reflects the interplay between the first-order spawning and second-order cancellation processes [25]. Similar to FCIQMC, our algorithm produces the correct nodal structure of the target state provided the total number of walkers exceeds a critical value N_c depending on a grid spacing, the dimension of configuration space and the character of the target state. Therefore, the value of N_c determines the memory footprint of the grid-based Monte-Carlo simulations. As a consequence of the fermion sign problem [15], N_c is expected to grow exponentially with the system size.

In this work we study the performance of our algorithm for a series of model problems and demonstrate that a steep growth of memory requirements with the grid spacing and system size restricts the scope of its applicability to the two-particle Coulomb systems in three-dimensional space.

The manuscript is structured as follows. We present a closed form-expression of the grid

propagator and a detailed description of our Monte-Carlo method in Sec. II. The results of benchmark calculations on fermions in harmonic traps, as well as singlet and triplet ground states of the helium atom, are reported in Sec. III A and Sec. III B, respectively. We conclude the paper with a brief overview of the computational aspects of the method and outline the directions of future work.

II. THEORY AND ALGORITHMS

We consider an N-particle Hamiltonian with a local spin-independent potential $V(r_1, r_2, ..., r_N)$:

$$H = -\frac{1}{2}\sum_{i=1}^{N}\Delta_i + V(r_1, r_2, ..., r_N) \tag{1}$$

We approximate the action of Laplacian operators on a uniform grid using a central three point finite difference formula:

$$\Delta_i = \Delta_i^{\delta} + O(\delta^2), \tag{2}$$

where δ is a grid spacing and Δ_i^{δ} is a symmetric lattice operator defined by the following expression (x_i, y_i, z_i is a set of spatial coordinates and s_i is a spin label of i-th electron):

$$\Delta_i^{\delta} f(x_i, y_i, z_i, s_i) = \frac{f(x_i+\delta, y_i, z_i, s_i) + f(x_i-\delta, y_i, z_i, s_i) - 2f(x_i, y_i, z_i, s_i)}{\delta^2} + \atop x_i \leftrightarrow y_i \leftrightarrow z_i \tag{3}$$

Replacing Δ_i with their lattice counterparts Δ_i^{δ} one can introduce a grid Hamiltonian H_{δ}. The action of the associated imaginary time propagator $e^{-\tau(H_{\delta}-\omega)}$ (ω and τ are energy onset and imaginary timestep, respectively) on a discretized wave function Ψ can be evaluated using Suzuki-Trotter formula [26] in the limit $\tau \to 0$:

$$\Psi_{\tau}(r_1, s_1; ...; r_N, s_N) = \sum_{d_1,...,d_N} \Omega_{d_1,...,d_N} \Psi(r_1 - d_1\delta, s_1; ...; r_N - d_N\delta, s_N) + O(\tau^2), \tag{4}$$

where $\Omega_{d_1,...,d_N}$ is a transition amplitude, defined as a product of a spawning factor $m_{d_1,...,d_N} = e^{-\tau\frac{V_0+V(...,x_i-d_i^x\delta,y_i-d_i^y\delta,z_i-d_i^z\delta,...)-2\omega}{2}}$ and a transition probability $P_{d_1,...,d_N} = \prod_{i=1}^{N} p_{d_i^x} p_{d_i^y} p_{d_i^z}$:

$$\Omega_{d_1,...,d_N} = m_{d_1,...,d_N} P_{d_1,...,d_N} = e^{-\tau\frac{V_0+V(...,x_i-d_i^x\delta,y_i-d_i^y\delta,z_i-d_i^z\delta,...)-2\omega}{2}} \prod_{i=1}^{N} p_{d_i^x} p_{d_i^y} p_{d_i^z}, \tag{5}$$

where $V_0 = V(r_1, ...r_N)$ is a value of the potential at the final point. The sum in Eq. 4 runs over all possible combinations of N three-dimensional lattice vectors d_i with integer coordinates. Factors p_d appearing in Eq. 5 can be calculated as follows:

$$p_d \;=\; \frac{1}{2\pi}\int_{-\pi}^{\pi} \cos(kd) e^{-\frac{2\tau}{\delta^2}\sin^2(k/2)} dk \tag{6}$$

As follows from its properties, p_d can be interpreted as a transition probability of a non-gaussian random walk on a one-dimensional lattice:

1. For $\tau = 0$ $p_d = \delta_{d0}$
2. $p_d \geq 0$
3. $\sum_{d=-\infty}^{\infty} p_d = \frac{1}{2\pi}\int_{-\pi}^{\pi}\sum_{d=-\infty}^{\infty} e^{ikd} e^{-\frac{2\tau}{\delta^2}\sin^2(k/2)} dk = \int_{-\pi}^{\pi} \delta(k) e^{-\frac{2\tau}{\delta^2}\sin^2(k/2)} dk = 1$

In the limit $\delta \to 0$, p_d converges to the transition probability of a diffusion random process in continuous space:

$$p_d \to \frac{1}{2\pi}\int_{-\infty}^{\infty} e^{ikd - \frac{1}{2\delta^2}\tau k^2} dk = \frac{\delta}{\sqrt{2\pi\tau}} e^{-\frac{d^2\delta^2}{2\tau}} \tag{7}$$

Eq. 7 follows from Eq. 6 by applying a saddle point approximation [27] to the integral in the vicinity of $k = 0$. Therefore, in the limit $\delta \to 0$ the lattice propagator reduces to the DMC evolution operator, which is consistent with $H_\delta \xrightarrow[\delta\to 0]{} H$.

The sum in Eq. 4 contains the terms that differ only by the interchange of particles with identical spin labels and are therefore equivalent up to the phase. This can be systematically accounted for by introducing a standard ordering of the grid nodes and permuting particle coordinates such that the list of occupied nodes conforms to the chosen order within the groups of particles with the same spin label.

Eq. 4 admits a stochastic interpretation similar to DMC with a major difference being due to the definition of random walkers and transition probability. In the following it is assumed that each walker represents a set of particle coordinates on an integer lattice and is carrying a unit weight $c = \pm 1$. The particles are assigned fixed spin labels s_i such that the spin projection S_z of a target state is $S_z = \sum_{i=1}^{N} s_i$. A random walker flips sign, whenever the exchange of two particles with the same spin label occurs in the course of propagation.The calculation work-flow is similar to that of DMC [9, 10] and includes the following steps:

1. **Initialization**. Initial walker positions are sampled from an N-particle discretized trial wave function $|\Psi_T(r_1, ..., r_N)|$. Sampling is performed using a standard Metropolis algorithm with a proposal distribution chosen to avoid potential singularities, if applicable. The initial walker weights are assigned according to the sign structure of Ψ_T.

2. **Transition probability calculation**. p_d factors are computed from Eq. 6 via numerical integration and are stored in a list along with the associated integer displacements d. This calculation is performed only once at the beginning of a Monte-Carlo run.

3. **Propagation and spawning**. Each walker performs a branching random walk with hopping probabilities $P_{d_1,...,d_N} = \prod_{i=1}^{N} p_{d_i^x} p_{d_i^y} p_{d_i^z}$. The propagation step is executed by looping over the list of walkers W and displacing walker coordinates by 3N dimensional vectors $(d_1, ..., d_N)$ sampled from $P_{d_1,...,d_N}$. If the new set of occupied grid points does not conform to a standard order, the particles are permuted accordingly, by applying a permutation P. The walker weight is then multiplied by $(-1)^{[P]}$, where $[P]$ is the parity of P. Examples of sign-flipping and sign-preserving moves are presented in Fig. 1 for a simple case of two fermions in two-dimensional space.

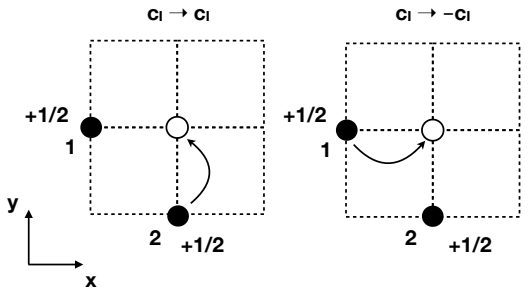

FIG. 1: Examples of sign-flipping (right panel) and sign-preserving (left panel) Monte-Carlo moves for two fermions with spin labels $s_i = +1/2$ (i = 1,2) in two-dimensional space. The grid nodes are assumed to follow dictionary order such that $(x, y) > (x', y')$ either if $x > x'$ or if $x = x'$ and $y > y'$.

After the coordinate update is completed for a given walker, the old $\vec{r}^{old} = (r_1^{old}, r_2^{old}, ..., r_N^{old})$ and the new set of the particle coordinates $\vec{r}^{new} = (r_1^{old} + d_1\delta, r_2^{old} + d_2\delta, ..., r_N^{old} + d_N\delta)$ are used to calculate the branching factor $m = e^{-\tau \frac{V(\vec{r}^{old}) + V(\vec{r}^{new}) - 2\omega}{2}}$.

The walker is subsequently replaced by $\lfloor m + \xi \rfloor$ copies, where ξ is a random number sampled for a uniform distribution on the interval $[0, 1]$.

4. **Annihilation**. The new list W' of walkers is sorted and searched for members occupying the same grid nodes. The weights of a group of walkers sharing the same grid point are summed to give a total weight g. The group is replaced by $|g|$ walkers with the weights equal to $sign(g)$.

5. **Measure the energy**. The energy offset ω is updated to keep the number of walkers approximately constant $\omega \rightarrow \omega + 1/\tau \ln[N(W)/N(W')]$, where $N(W)$ and $N(W')$ are the sizes of the old and new walker lists, respectively. The mean value of ω in the limit $\tau \rightarrow \infty$ can be used to estimate the ground state energy (growth estimator [28], $E_{gr} = \langle \omega \rangle$). Statistical accuracy considerations suggest that it is desirable to have another measure of the total energy (projected estimator [16, 29], E_{proj}) defined as follows:

$$E_{proj}(\tau) = \frac{\sum_i H_\delta \Psi_T(r_1^i, ...r_N^i) c_i}{\sum_i \Psi_T(r_1^i, ...r_N^i) c_i}, \tag{8}$$

where r_k^i represents a position of k-th particle associated with i-th walker, c_i is a corresponding weight and Ψ_T is a trial function having a non-zero overlap the target state.

A branching random walk defined by the above algorithm samples the ground state of H_δ as the total propagation time approaches infinity. For large walker ensembles, the computational cost of a Monte-Carlo iteration is dominated by walker annihilation step which exhibits $N_w \log(N_w)$ scaling with the number of walkers N_w due to the need to sort the walker list and presents an obstacle to a scalable parallel implementation of the algorithm. We note, however, that the estimate should be viewed as an upper bound as it ignores the fact that only a fraction of walkers gets displaced at each Monte-Caro step. As will be shown in the next section, one of the important implications of the walker annihilation is the existence of the critical ensemble size N_c required to converge the nodal structure of the target state. The value of N_c defines the memory footprint of the algorithm and restricts the size of systems that can be simulated. The lack of cancellation for small walker ensembles, i.e. $N_w < N_c$, leads to node sampling errors and introduces a bias in calculated energy [16].

III. RESULTS AND DISCUSSION

The performance of the method was studied for a series of model problems with the focus on the two-particle systems in three-dimensional space in view of potential applications in the context of real space MP2 and CC2 calculations. In all cases transition probabilities p_d were calculated numerically using Clenshaw-Curtis adaptive quadrature algorithms implemented in GNU scientific library [30]. Displacements with the probabilities $\leq 10^{-8}$ were discarded. The spatial grid was chosen to have the same spacing along X, Y and Z directions. Statistical errors of the energy estimators were evaluated using blocking analysis [31] as implemented in pyblock module [32].

A. Fermions in Harmonic traps

We considered a system of four independent spin-1/2 particles confined in a one dimensional harmonic trap represented by a potential of the form $V = 1/2 \sum_{i=1}^{4} x_i^2$, where x_i are particle coordinates. The algorithm of Sec. II was used to sample the ground states of the system with the total spin S equal to 0, 1, and 2. The simulation was performed on a grid with spacing $\delta = 0.1$ a.u. The initial particle positions were sampled from a uniform distribution within a 6.0 a.u. cubic box. The ensemble of $\sim 10^7$ random walkers was propagated for the total of 5000 Monte-Carlo steps with the imaginary time step 0.1 a.u. Upon convergence, the target state energy was measured by the growth estimator. The main sources of error in the calculated energies were due to the finite time step and non-zero grid spacing, the latter precluding direct comparison with the known exact results in continuous space. Consequently, reference energy values were evaluated as the sums of one particle energies obtained by diagonalizing discretized harmonic oscillator Hamiltonian on a uniform grid spanning the interval $[-L, L]$, where $L =$ 6.0 a.u., and were converged up to at least eight decimal places with respect to L. As shown in Table I, the differences between Monte-Carlo energy estimates and the reference values are within 3 mH which can be attributed to the time step error.

In order to study the effect of the cancellation rate on the Monte-Carlo energy estimates we performed a series of runs for the walker ensembles of varying sizes. The simulation results presented in Fig. 2 (Panel A) indicate that the energies converge to reference values provided the frequency of cancellation events or, equivalently, the total number of walkers exceeds a

TABLE I: Energies of the spin states of the four particle (spin-1/2) fermion system in a 1-D harmonic trap (grid spacing 0.1 a.u.). See the main text for the simulation details.

Spin	E_{gr}, a.u.	E_{exact}, a.u.
0	3.99458 ± 0.00004	3.996246
1	4.99168 ± 0.00004	4.993740
2	7.98292 ± 0.00005	7.986223

threshold value N_c depending on the character of the target state. The lack of cancellation manifests itself in the values of the growth estimator below the true ground state energy. The rate of convergence tends to decrease for high spin states. The population dynamics curves presented in Fig. 2 (Panel B) are reminiscent of those obtained in FCIQMC [16] and similarly exhibit pronounced plateaus corresponding to N_c values. This feature reflects the competition between the spawning and walker cancellation process [25].

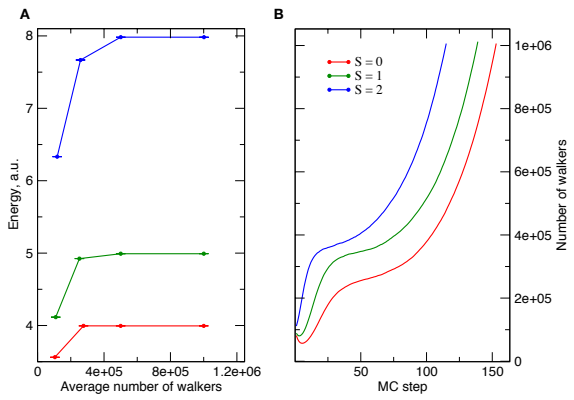

FIG. 2: The dependence of the growth estimator on the average number of walkers for the lowest spin states of the four fermions in a one-dimensional harmonic trap (A). The typical population dynamics pattern in a grid-based quantum Monte-Carlo run. The energy onset was set to 4.25, 5.25, and 8.25 for the states with spin 0, 1, and 2, respectively and kept fixed during the propagation (B).

The grid dependence of N_c was further analyzed for a triplet system of two spin-1/2 fermions in a 3-D harmonic trap. Due to the larger dimension of the configuration space N_c is an order of magnitude larger compared to the previously considered system and exhibits a steep growth

with δ (Fig. 3). The least square fit of the $\ln N_c$ - $\ln \delta$ dependence suggests that $N_c \approx 339\delta^{-5.994}$. In general, one could expect $N_c \propto \delta^{-Nd}$, where N is the number of particles and d is the dimension of one-particle configuration space.

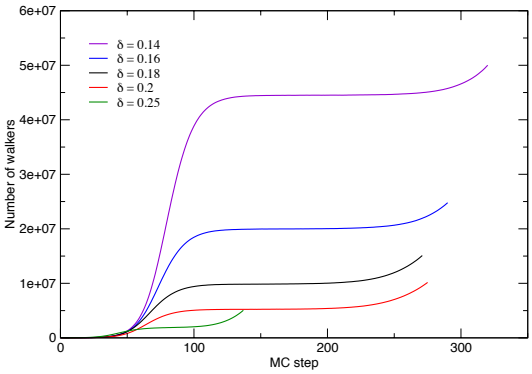

FIG. 3: Population dynamics for two spin-1/2 fermions in a 3-D harmonic trap for several grid spacings δ. The calculations were performed for the energy onset $\omega = 4.5$ a.u. and imaginary time-step $\delta t = 0.1$ a.u.

B. ^1S and ^3S states of Helium atom

Monte-Carlo simulation of Coulomb systems requires modifications of the algorithm to account for the singularities of the potential energy operator. In contrast to continuous DMC, random walks in discretized space have a non-zero probability of visiting coincidence planes (i.e. the regions of space where $r_i = r_j$ for some pair of electrons) as well as electron-nucleus coalescence points, leading to the diverging branching factors. In order to avoid divergences, we placed the nucleus of He atom at the point with coordinates $(\delta/2, \delta/2, \delta/2)$, where δ is the grid spacing, and terminated the random walks whenever the electron coordinates coincided. The reference energy values were obtained from the fixed-node grid-based Monte-Carlo simulations using a known exact nodal surface of the ^3S state [33]. The nodal constraint was imposed by killing random walkers attempting to acquire a sign inconsistent with that of a trial wave function Ψ_T having exact node, i.e. the walker weight c_i was set to 0 if $c_i \times \Psi_T(r_1^i, r_2^i) < 0$

Simulations were performed for the ensemble of 10000 walkers and imaginary time step 0.005

a.u. The energy was measured by the projection estimator as described in Sec II. The results of the grid-based fixed-node calculations on the ^3S state of He atom are presented in Fig. 4 (Left panel).

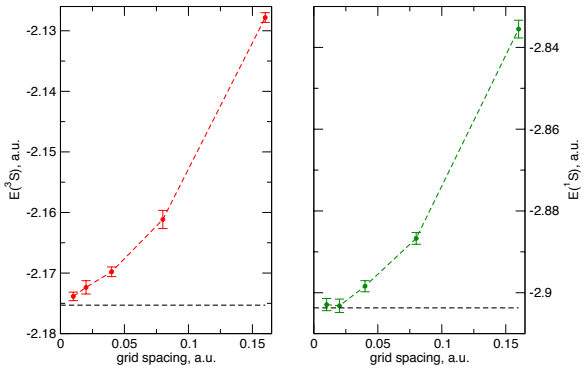

FIG. 4: Energies of the ^3S (Left panel) and ^1S (Right panel) states of He atom as a functions of grid spacing. Statistical errors are shown with vertical bars. Horizontal dashed lines indicate Pekeris results [34].

Fixed-node energy of the ^3S state of He exhibits slow convergence with the grid spacing, being in error of 1.5 mH with respect to the reference value [34] even for $\delta = 0.01$ a.u. Comparison with the similar simulation for ^1S state (Fig. 4, Right panel) suggests that this can be attributed to the inherent inefficiency of a uniform grid in representing electron-nuclear and to lesser extent electron-electron cusps [2]. Interestingly, the grid acts to suppress the fluctuations of the branching factor by preventing the walkers from closely approaching the nucleus and gives rise to the order of magnitude smaller statistical errors compared to similar continuous space calculations [24]. Note, that the bias due to the finite grid spacing appears to decrease monotonously with δ in the range from 0.16 to 0.01 a.u. For finer grids the character of convergence is hard to discern as it is masked by statistical errors.

Grid-based Monte-Carlo simulations beyond fixed-node approximation were performed for two grid spacings, $\delta = 0.16$ and $\delta = 0.08$. In both cases the convergence with respect to the number of walkers was ensured by performing the calculation for walker ensembles of varying sizes and checking the stability of the energy estimates. Additionally, the average fraction of walkers w with correct signs (i.e. with the sign consistent with Ψ_T) was recorded during

Monte-Carlo runs to quantify the accuracy of the nodal structure. The calculation results are presented in Table. II along with the fixed-node energies for the same grid spacings.

TABLE II: Energies of the ^3S state of He atom obtained from grid-based DMC calculations without nodal constraints. Fixed-node results are presented for reference purposes.

δ	$< N >$	w	E, a.u.	fixed node
0.16	35027070	0.979	-2.12695 $\pm$ 10^{-5}	N
0.16	70489775	0.983	-2.12687 $\pm$ 10^{-5}	N
0.16	10000	1.00	-2.1278 $\pm$ 0.001	Y
0.08	615787933	0.967	-2.16126 $\pm$ 10^{-5}	N
0.08	625057844	0.968	-2.16169 $\pm$ 10^{-5}	N
0.08	10008	1.00	-2.1612 $\pm$ 0.0015	Y

The values of w close to 1.0 indicate the convergence of the Monte-Carlo iteration to the state with nearly exact nodal structure. Energy estimates obtained from the simulations without nodal constraints are in excellent agreement with the reference fixed-node results within the statistical error bars. The critical number of walkers in our simulations exceeded $\sim 6 \times 10^8$ for the case of the fine grid ($\delta = 0.08$ a.u.). Yet, in order to reduce the grid bias to a sub-millihartree level even finer grids (with $\delta < 0.04$ a.u.) are required (Fig. 4). The estimated critical number of walkers for such simulations would however exceed 3.8×10^{10} rendering them unfeasible due to the large memory requirements.

IV. SUMMARY AND CONCLUSIONS

We developed a novel grid-based algorithm enabling quantum Monte-Carlo simulations of the target states with arbitrary nodal structure without invoking the fixed-node approximation. To this end, the original continuous space problem was mapped onto its lattice fermion counterpart by representing the Hamiltonian on the infinite uniform spatial grid using a central finite difference approximation for the kinetic energy operator. We showed that the associated grid propagator is similar to that of the continuous space diffusion Monte-Carlo and reduces to it in the limit of zero grid spacing, yet describes a non-gaussian statistics of walker moves.

The key component of the formalism is the definition of random walkers which incorporates the permutational symmetry of the target state and can be extended to account for the point group symmetries. For a series of model systems we demonstrated that our Monte-Carlo algorithm converges to target states with the correct nodal structure, provided the total number of walkers exceeds a critical value N_c. The latter determines the memory footprint of the method and restricts the scope of its applicability to the two particle Coulomb systems in three-dimensional space as well as some low-dimensional model problems with smooth potentials. As follows from the simulation results for the triplet state of He atom, realistic grid based Monte-Carlo calculations on atoms can require as many as $10^7 - 10^9$ walkers to achieve moderate accuracy of the energy estimates. This can be attributed to the inefficient representation of the electron-nucleus cusp on a uniform Cartesian grid. The memory requirements for our Monte-Carlo simulations on the triplet state of He did not exceed ~ 17 Gb of RAM. Further reduction of the bias in calculated energy would require a several orders of magnitude larger amount of memory and would be problematic even for a distributed multi-node system. We note however that smooth convergence of the error with the grid spacing can be harnessed to develop efficient extrapolation schemes [7]. Furthermore, the memory requirements can be reduced by utilizing spatial symmetry and extending the algorithm for the case of adaptive grids, which is currently under active development.

V. ACKNOWLEDGMENTS

This work was supported by the U.S. Department of Energy, Office of Science, Basic Energy Sciences as part of the Computational Chemical Sciences Program. The author gratefully acknowledges helpful discussions with Prof. So Hirata and Prof. David Ceperley.

VI. SUPPLEMENTARY INFORMATION

The reference Python implementation of the Monte-Carlo algorithm presented in the paper is available on `https://github.com/aakunitsa/QMC\_grid\_theory.git`

[1] O. Sinanolu, J. Chem. Phys. **36**, 3198 (1962).

[2] F. A. Bischoff and E. F. Valeev, J. Chem. Phys. **139**, 114106 (2013).

[3] S. Hirata, T. Shiozaki, C. M. Johnson, and J. D. Talman, Mol. Phys. **115**, 510 (2017).

[4] J. S. Kottmann and F. A. Bischoff, J. Chem. Theory Comput. **13**, 5945 (2017), URL https://doi.org/10.1021/acs.jctc.7b00694.

[5] T. Yanai, G. I. Fann, Z. Gan, R. J. Harrison, and G. Beylkin, J. Chem. Phys. **121**, 6680 (2004), URL https://aip.scitation.org/doi/abs/10.1063/1.1790931.

[6] R. J. Harrison, G. I. Fann, T. Yanai, Z. Gan, and G. Beylkin, J. Chem. Phys. **121**, 11587 (2004).

[7] V. McKoy and N. W. Winter, J. Chem. Phys. **48**, 5514 (1968), ISSN 0021-9606, URL https://aip.scitation.org/doi/abs/10.1063/1.1668249.

[8] M. H. Kalos, Phys. Rev. **128**, 1791 (1962), URL http://link.aps.org/doi/10.1103/PhysRev.128.1791.

[9] J. B. Anderson, J. Chem. Phys. **63**, 1499 (1975), ISSN 0021-9606, 1089-7690, URL http://scitation.aip.org/content/aip/journal/jcp/63/4/10.1063/1.431514.

[10] A. Lchow, WIREs Comput Mol Sci **1**, 388 (2011), ISSN 1759-0884, URL http://onlinelibrary.wiley.com/doi/10.1002/wcms.40/abstract.

[11] Michele Casula, Claudia Filippi, and Sandro Sorella, Phys. Rev. Lett. **95**, 100201 (2005).

[12] M. Casula, S. Moroni, S. Sorella, and C. Filippi, J. Chem. Phys. **132**, 154113 (2010).

[13] Peter J. Reynolds and David M. Ceperley, J. Chem. Phys. **77**, 5593 (1982), ISSN 0021-9606, URL http://aip.scitation.org/doi/abs/10.1063/1.443766.

[14] D. J. Klein and H. M. Pickett, J. Chem. Phys. **64**, 4811 (1976), ISSN 0021-9606, 1089-7690, URL http://scitation.aip.org/content/aip/journal/jcp/64/11/10.1063/1.432043.

[15] M. Troyer and U.-J. Wiese, Phys. Rev. Lett. **94**, 170201 (2005).

[16] George H. Booth, Alex J. W. Thom, and Ali Alavi, J. Chem. Phys. **131**, 054106 (2009), ISSN 0021-9606, URL http://aip.scitation.org/doi/full/10.1063/1.3193710.

[17] D. Cleland, G. H. Booth, and A. Alavi, J. Chem. Phys. **132**, 041103 (2010), ISSN 0021-9606, URL http://aip.scitation.org/doi/10.1063/1.3302277.

[18] J. Carlson and M. H. Kalos, Phys. Rev. C **32**, 1735 (1985), URL http://link.aps.org/doi/10.1103/PhysRevC.32.1735.

[19] M. H. Kalos and K. E. Schmidt, J. Stat. Phys. **89**, 425 (1997), ISSN 0022-4715, 1572-9613, URL http://link.springer.com/article/10.1007/BF02770774.

[20] M. H. Kalos, Phys. Rev. E **53**, 5420 (1996), URL http://link.aps.org/doi/10.1103/PhysRevE.53.5420.

[21] M. H. Kalos and F. Pederiva, Phys. Rev. Lett. **85**, 3547 (2000), URL https://link.aps.org/doi/10.1103/PhysRevLett.85.3547.

[22] James B. Anderson, Carol A. Traynor, and Bruce M. Boghosian, J. Chem. Phys. **95**, 7418 (1991), ISSN 0021-9606, 1089-7690, URL http://scitation.aip.org/content/aip/journal/jcp/95/10/10.1063/1.461368.

[23] Y. Mishchenko, Phys. Rev. E **73**, 026706 (2006), URL http://link.aps.org/doi/10.1103/PhysRevE.73.026706.

[24] D. Coker and R. O. Watts, Mol. Phys. **58**, 1113 (1986).

[25] Spenser J. S., J. Chem. Phys. **136**, 054110 (2012), ISSN 0021-9606, URL http://aip.scitation.org/doi/10.1063/1.3681396.

[26] H. F. Trotter, Proc. Amer. Math. Soc. **10**, 545 (1959), URL https://mathscinet.ams.org/mathscinet-getitem?mr=0108732.

[27] J. Mathews and R. L. Walker, *Mathematical Methods of Physics* (W.A. Benjamin, New York, 1970), 2nd ed., ISBN 978-0-8053-7002-7.

[28] C. J. Umrigar, M. P. Nightingale, and K. J. Runge, J. Chem. Phys. **99**, 2865 (1993), ISSN 0021-9606, URL http://aip.scitation.org/doi/abs/10.1063/1.465195.

[29] G. An and J. M. J. van Leeuwen, Phys. Rev. B **44**, 9410 (1991), URL http://link.aps.org/doi/10.1103/PhysRevB.44.9410.

[30] M. G. et al., *Gnu scientific library reference manual (3rd ed.)*, URL http://www.gnu.org/software/gsl/.

[31] H. Flyvbjerg and H. G. Petersen, J. Chem. Phys. **91**, 461 (1989).

[32] J. Spencer, *pyblock: python module for performing blocking analysis on data containing serial correlations*, original-date: 2014-04-02T02:12:30Z, URL https://github.com/jsspencer/pyblock.

[33] Dario Bressanini and Peter J. Reynolds, Phys. Rev. Lett. **95**, 110201 (2005).

[34] C. L. Pekeris, Phys. Rev. **126**, 1470 (1962).